about the origin must balance the concentrated line force, which has unit magnitude

$$1 = \int_0^{2\pi} \tilde{\sigma}_{3r} r \, \mathrm{d}\theta = 2\pi\mu A. \tag{3.31}$$

Thus, $A = 1/2\pi\mu$, and the Green's function is

$$\tilde{g}_3^3 = \frac{1}{2\pi\mu} \ln r = \frac{1}{2\pi\mu} \ln \sqrt{(\xi_1 - x_1)^2 + (\xi_2 + x_2)^2}. \tag{3.32}$$

Here, the point source has been offset from the origin to the point $(x_1, -x_2)$. The horizontal shear stress is

$$\tilde{\sigma}_{23}^3 = \mu \frac{\partial \tilde{g}_3^3}{\partial x_2} = \frac{1}{2\pi} \frac{\xi_2 + x_2}{(\xi_1 - x_1)^2 + (\xi_2 + x_2)^2}, \tag{3.33}$$

which does not match the free-surface boundary condition $\tilde{\sigma}_{23}(\xi_2 = 0) = 0$. However, adding an image source of the same sign at (x_1, x_2) does cause the shear stress to vanish.

Equation (3.27) involves the shear stress $\tilde{\sigma}_{13}^3$ acting on the fault surface, which we take to be the plane $\xi_1 = 0$. Including the concentrated line force and its image,

$$\tilde{\sigma}_{13}^3 = -\frac{1}{2\pi} \left[\frac{x_1}{x_1^2 + (\xi_2 + x_2)^2} + \frac{x_1}{x_1^2 + (\xi_2 - x_2)^2} \right]. \tag{3.34}$$

If we measure the displacement only on the free surface, then $x_2 = 0$, and equation (3.27) becomes

$$u_3(x_1, x_2 = 0) = -\frac{1}{\pi} \int_{-\infty}^{0} s_3(\xi_2) \frac{x_1}{x_1^2 + \xi_2^2} \mathrm{d}\xi_2, \tag{3.35}$$

which is consistent with equation (2.41).

3.3 Two-Dimensional Edge Dislocations

In order to use Volterra's formula to compute the displacements due to an infinitely long edge dislocation, we require the plane strain Green's functions. These correspond to the displacements from a concentrated line force acting in the plane. Rather than derive the result as for the antiplane strain case earlier, we make use of Melan's (1932; note correction in 1940) results. (See also Dundurs [1962], who gives results for concentrated line forces in joined elastic half-planes; the half-plane is a special case in which the shear modulus of the region not containing the localized line force vanishes.)

The Green's functions could be derived starting from the well-known solution for a concentrated force in a full-plane (Love 1944, article 148). An image source of the same sign located symmetrically about the plane $x_2 = 0$ cancels one component of the traction acting on $x_2 = 0$. The problem then is to remove the remaining traction component. Melan's approach is to use the result for a concentrated force acting on the boundary of a half-plane. An appropriative distribution of such forces is constructed that exactly cancels the tractions from the full-space line force and its image. An alternative approach is to use Fourier transform methods to remove the resulting tractions. Such an approach is used in section 10.6 to derive the solution for a

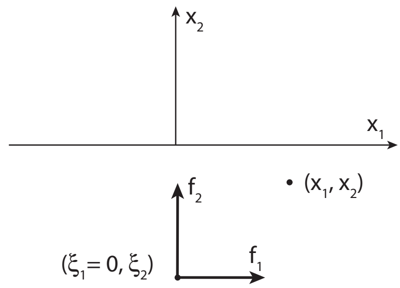

Figure 3.7. Line forces at $(0, \xi_2)$, extending infinitely in the 3-direction, give rise to displacements measured at (x_1, x_2).

line center of dilatation, a simple model of an expanding magma chamber, in a poroelastic half-plane.

For a line force in the x_1 direction, the displacements at (x_1, x_2) resulting from a line force acting at $(0, \xi_2)$ (figure 3.7) are

$$g_1^1 = \frac{-1}{2\pi\mu(1-\nu)}\left[\frac{3-4\nu}{4}\ln r_1 + \frac{8\nu^2-12\nu+5}{4}\ln r_2 + \frac{(x_2-\xi_2)^2}{4r_1^2} + \frac{(3-4\nu)(x_2+\xi_2)^2 + 2\xi_2(x_2+\xi_2) - 2\xi_2^2}{4r_2^2} - \frac{\xi_2 x_2 (x_2+\xi_2)^2}{r_2^4}\right], \tag{3.36}$$

$$g_2^1 = \frac{1}{2\pi\mu(1-\nu)}\left[(1-2\nu)(1-\nu)\theta_2 + \frac{(x_2-\xi_2)x_1}{4r_1^2} + (3-4\nu)\frac{(x_2-\xi_2)x_1}{4r_2^2} - \frac{\xi_2 x_2 x_1 (x_2+\xi_2)}{r_2^4}\right]. \tag{3.37}$$

For a line force in the x_2 direction,

$$g_1^2 = \frac{1}{2\pi\mu(1-\nu)}\left[-(1-2\nu)(1-\nu)\theta_2 + \frac{(x_2-\xi_2)x_1}{4r_1^2} + (3-4\nu)\frac{(x_2-\xi_2)x_1}{4r_2^2} + \frac{\xi_2 x_2 x_1 (x_2+\xi_2)}{r_2^4}\right], \tag{3.38}$$

$$g_2^2 = \frac{1}{2\pi\mu(1-\nu)}\left[-\frac{3-4\nu}{4}\ln r_1 - \frac{8\nu^2-12\nu+5}{4}\ln r_2 - \frac{x_1^2}{4r_1^2} + \frac{2\xi_2 x_2 - (3-4\nu)x_1^2}{4r_2^2} - \frac{\xi_2 x_2 x_1^2}{r_2^4}\right], \tag{3.39}$$

where

$$\begin{aligned} r_1^2 &= x_1^2 + (x_2-\xi_2)^2, \\ r_2^2 &= x_1^2 + (x_2+\xi_2)^2, \end{aligned} \tag{3.40}$$

and

$$\theta_2 = \tan^{-1}\left(\frac{x_1-\xi_1}{x_2+\xi_2}\right). \tag{3.41}$$

Note that if the line force is located at $x_1 = \xi_1$ rather than at $x_1 = 0$, we simply replace x_1 with $x_1 - \xi_1$.

For a line force in the x_1 direction, the corresponding stresses are

$$\sigma_{11}^{1} = \frac{-1}{2\pi\,(1-\nu)}\left\{\frac{x_1^3}{r_1^4} + \frac{x_1\left(x_1^2 - 4\xi_2 x_2 - 2\xi_2^2\right)}{r_2^4} + \frac{8\xi_2 x_2 x_1\,(x_2+\xi_2)^2}{r_2^6} + \frac{1-2\nu}{2}\left[\frac{x_1}{r_1^2} + \frac{3x_1}{r_2^2} - \frac{4x_2 x_1\,(x_2+\xi_2)}{r_2^4}\right]\right\}, \tag{3.42}$$

$$\sigma_{12}^{1} = \frac{-1}{2\pi\,(1-\nu)}\left\{\frac{(x_2-\xi_2)\,x_1^2}{r_1^4} + \frac{(x_2+\xi_2)\left(2\xi_2 x_2 + x_1^2\right)}{r_2^4} - \frac{8\xi_2 x_2 x_1^2\,(x_2+\xi_2)}{r_2^6} + \frac{1-2\nu}{2}\left[\frac{x_2-\xi_2}{r_1^2} + \frac{3x_2+\xi_2}{r_2^2} - \frac{4x_2\,(x_2+\xi_2)^2}{r_2^4}\right]\right\}, \tag{3.43}$$

$$\sigma_{22}^{1} = \frac{-1}{2\pi\,(1-\nu)}\left\{\frac{(x_2-\xi_2)^2\,x_1}{r_1^4} - \frac{x_1\left(\xi_2^2 - x_2^2 + 6\xi_2 x_2\right)}{r_2^4} + \frac{8\xi_2 x_2 x_1^3}{r_2^6} - \frac{1-2\nu}{2}\left[\frac{x_1}{r_1^2} - \frac{x_1}{r_2^2} - \frac{4x_2 x_1\,(x_2+\xi_2)}{r_2^4}\right]\right\}. \tag{3.44}$$

For a line force in the x_2 direction,

$$\sigma_{11}^{2} = \frac{-1}{2\pi\,(1-\nu)}\left\{\frac{(x_2-\xi_2)\,x_1^2}{r_1^4} + \frac{(x_2+\xi_2)\left(x_1^2 + 2\xi_2^2\right) - 2\xi_2 x_1^2}{r_2^4} + \frac{8\xi_2 x_2\,(x_2+\xi_2)\,x_1^2}{r_2^6}, + \frac{1-2\nu}{2}\left[-\frac{x_2-\xi_2}{r_1^2} + \frac{3\xi_2+x_2}{r_2^2} + \frac{4x_2 x_1^2}{r_2^4}\right]\right\}, \tag{3.45}$$

$$\sigma_{12}^{2} = \frac{-x_1}{2\pi\,(1-\nu)}\left\{\frac{(x_2-\xi_2)^2}{r_1^4} + \frac{x_2^2 - 2\xi_2 x_2 - \xi_2^2}{r_2^4} + \frac{8\xi_2 x_2\,(x_2+\xi_2)^2}{r_2^6} + \frac{1-2\nu}{2}\left[\frac{1}{r_1^2} - \frac{1}{r_2^2} + \frac{4x_2\,(x_2+\xi_2)}{r_2^4}\right]\right\}, \tag{3.46}$$

$$\sigma_{22}^{2} = \frac{-1}{2\pi\,(1-\nu)}\left\{\frac{(x_2-\xi_2)^3}{r_1^4} + \frac{(x_2+\xi_2)\left[(x_2+\xi_2)^2 + 2\xi_2 x_2\right]}{r_2^4} - \frac{8\xi_2 x_2\,(x_2+\xi_2)\,x_1^2}{r_2^6} + \frac{1-2\nu}{2}\left[\frac{x_2-\xi_2}{r_1^2} + \frac{3x_2+\xi_2}{r_2^2} - \frac{4x_2 x_1^2}{r_2^4}\right]\right\}. \tag{3.47}$$

We are now in a position to evaluate the displacements for dip-slip faults. For simplicity, observation points are restricted to the free surface where field measurements are collected. Volterra's formula (3.6) requires the stress acting on the fault due to a line force acting at the observation point. In the Melan solution, the line force is applied at $\boldsymbol{\xi}$, and the stress is resolved at $\mathbf{x}$. To be consistent with our notation for Volterra's formula, we swap $\mathbf{x}$ and $\boldsymbol{\xi}$ in equation (3.6). For a vertical fault $n_j = \delta_{1j}$ and $s_i = s\delta_{2i}$, so with the current notation, equation (3.6) becomes

$$u_k(\xi_1, \xi_2 = 0) = \int s(x_2)\tilde{\sigma}_{12}^{k}(x_1, x_2; \xi_1, \xi_2 = 0)\mathrm{d}x_2 \quad k = 1, 2. \tag{3.48}$$

As in section 3.2, we have integrated the point force solution along x_3 to produce a line source. The tilde notation is dropped in the following; however, it should be understood that displacement and stress Green's functions are associated with line sources rather than point sources. Given that observations are restricted to the free surface, we simplify Melan's solution for a line source acting on the free surface $\xi_2 = 0$:

$$\sigma_{12}^{1}(\xi_1, \xi_2 = 0) = -\frac{2}{\pi}\frac{(x_1 - \xi_1)^2 x_2}{[(x_1 - \xi_1)^2 + x_2^2]^2} \tag{3.49}$$

$$\sigma_{12}^{2}(\xi_1, \xi_2 = 0) = -\frac{2}{\pi}\frac{(x_1 - \xi_1) x_2^2}{[(x_1 - \xi_1)^2 + x_2^2]^2}. \tag{3.50}$$

For a vertical fault located at the origin of the coordinate system, take $x_1 = 0$, without loss of generality, and $x_2 = z$, where z is the dummy variable on the fault surface. Assuming uniform slip below depth d, substituting equation (3.50) into (3.48) and integrating leads to

$$\begin{aligned} u_1(\xi_1, \xi_2 = 0) &= \frac{-2s\xi_1^2}{\pi}\int_{-\infty}^{-d}\frac{z}{(\xi_1^2 + z^2)^2}\mathrm{d}z, \\ &= \frac{2s\xi_1^2}{\pi}\left[\frac{1}{2(\xi_1^2 + z^2)}\right]_{z=-\infty}^{z=-d}, \\ &= \frac{s}{\pi}\frac{\xi_1^2}{\xi_1^2 + d^2}. \end{aligned} \tag{3.51}$$

For the vertical component of displacement due to slip on a vertical fault,

$$\begin{aligned} u_2(\xi_1, \xi_2 = 0) &= \frac{2s\xi_1}{\pi}\int_{-\infty}^{-d}\frac{z^2}{(\xi_1^2 + z^2)^2}\mathrm{d}z, \\ &= \frac{2s\xi_1}{\pi}\left[\frac{-z}{2(\xi_1^2 + z^2)} + \frac{1}{2\xi_1}\tan^{-1}\left(\frac{z}{\xi_1}\right)\right]_{z=-\infty}^{z=-d}, \\ &= \frac{s}{\pi}\left[\frac{\xi_1 d}{\xi_1^2 + d^2} + \tan^{-1}\left(\frac{\xi_1}{d}\right)\right]. \end{aligned} \tag{3.52}$$

Notice that the horizontal displacement u_1 goes to s/π for $|\xi_1| \gg d$. We can remove this rigid body motion, without affecting the stresses or strains. After doing so and introducing a distance parameter scaled by the fault depth $\zeta = \xi_1/d$, we have

$$\begin{aligned} u_1 &= -\frac{s}{\pi}\frac{1}{1 + \zeta^2}, \\ u_2 &= \frac{s}{\pi}\left[\frac{\zeta}{1 + \zeta^2} + \tan^{-1}(\zeta)\right]. \end{aligned} \tag{3.53}$$

3.3.1 Dipping Fault

We now consider the more general case of a fault dipping at an angle δ with respect to the horizontal. The most direct way to derive the displacements at the free surface is to compute the displacements for a horizontal dislocation (see problem 2). The displacements due to a dipping dislocation are found by a vector sum of the horizontal and vertical components of the slip vector (see problem 3). Vector summation of the two components is valid because, as has been emphasized earlier, the dislocation line is the source of deformation, not the dislocation plane. This approach is not valid for the displacements within the earth, however, where we we must ensure that the branch cut coincides with the dislocation surface.

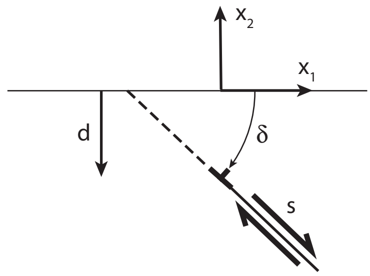

Figure 3.8. Geometry for a dipping edge dislocation in a half-space. The dislocation line, corresponding to the top of the fault, is at depth d, and the dislocation dips at angle δ from the free surface.

Here we will examine a more general, if somewhat more involved, approach using the double-couple form of Volterra's formula that is valid everywhere, not only at the free surface. From figure 3.8, the fault normal is $\mathbf{n} = [\sin\delta, \cos\delta, 0]^T$, and the fault slip is $\mathbf{s} = s[\cos\delta, -\sin\delta, 0]^T$.

Assuming constant slip over a confined interval, equation (3.15) becomes

$$\begin{aligned} u_k(\mathbf{x}) &= \mu s \int \left[2\sin\delta\cos\delta \left(\frac{\partial g_k^1}{\partial \xi_1} - \frac{\partial g_k^2}{\partial \xi_2} \right) + (\cos^2\delta - \sin^2\delta) \left(\frac{\partial g_k^1}{\partial \xi_2} + \frac{\partial g_k^2}{\partial \xi_1} \right) \right] d\Sigma, \\ &= \mu s \int \left[\sin 2\delta \left(\frac{\partial g_k^1}{\partial \xi_1} - \frac{\partial g_k^2}{\partial \xi_2} \right) + \cos 2\delta \left(\frac{\partial g_k^1}{\partial \xi_2} + \frac{\partial g_k^2}{\partial \xi_1} \right) \right] d\Sigma. \end{aligned} \tag{3.54}$$

The derivatives of the plane strain Green's tensors for displacements in the x_1 direction, evaluated at the free surface ($x_2 = 0$), are

$$\begin{aligned} \frac{\partial g_1^1}{\partial \xi_1} &= \frac{-1}{\pi\mu} \left\{ \frac{(x_1-\xi_1)[\nu\xi_2^2 - (1-\nu)(x_1-\xi_1)^2]}{[(x_1-\xi_1)^2+\xi_2^2]^2} \right\}, \\ \frac{\partial g_1^1}{\partial \xi_2} &= \frac{-1}{\pi\mu} \left\{ \frac{\xi_2[(2-\nu)(x_1-\xi_1)^2 + (1-\nu)\xi_2^2]}{[(x_1-\xi_1)^2+\xi_2^2]^2} \right\}, \\ \frac{\partial g_1^2}{\partial \xi_1} &= \frac{1}{\pi\mu} \left\{ \frac{\xi_2[(1-\nu)\xi_2^2 - \nu(x_1-\xi_1)^2]}{[(x_1-\xi_1)^2+\xi_2^2]^2} \right\}, \\ \frac{\partial g_1^2}{\partial \xi_2} &= \frac{1}{\pi\mu} \left\{ \frac{(x_1-\xi_1)[(1-\nu)\xi_2^2 - \nu(x_1-\xi_1)^2]}{[(x_1-\xi_1)^2+\xi_2^2]^2} \right\}, \end{aligned} \tag{3.55}$$

whereas displacements in the x_2 direction are

$$\begin{aligned} \frac{\partial g_2^1}{\partial \xi_1} &= \frac{1}{\pi\mu} \left\{ \frac{\xi_2[\nu\xi_2^2 - (1-\nu)(x_1-\xi_1)^2]}{[(x_1-\xi_1)^2+\xi_2^2]^2} \right\}, \\ \frac{\partial g_2^1}{\partial \xi_2} &= \frac{1}{\pi\mu} \left\{ \frac{(x_1-\xi_1)[\nu\xi_2^2 - (1-\nu)(x_1-\xi_1)^2]}{[(x_1-\xi_1)^2+\xi_2^2]^2} \right\}, \\ \frac{\partial g_2^2}{\partial \xi_1} &= \frac{1}{\pi\mu} \left\{ \frac{(x_1-\xi_1)[(1-\nu)(x_1-\xi_1)^2 + (2-\nu)\xi_2^2]}{[(x_1-\xi_1)^2+\xi_2^2]^2} \right\}, \\ \frac{\partial g_2^2}{\partial \xi_2} &= \frac{-1}{\pi\mu} \left\{ \frac{\xi_2[(1-\nu)\xi_2^2 - \nu(x_1-\xi_1)^2]}{[(x_1-\xi_1)^2+\xi_2^2]^2} \right\}. \end{aligned} \tag{3.56}$$

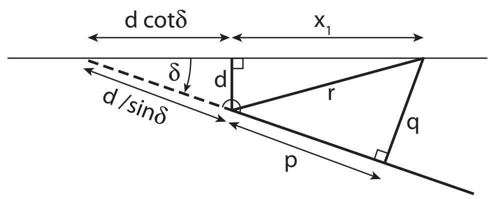

Figure 3.9. Coordinate system in which the vector from the fault to the observation point r is decomposed into perpendicular component q and parallel component p.

Combining with preceding equations (3.54) yields

$$\begin{aligned} u_1 &= \frac{s}{\pi} \int \sin 2\delta \left[\frac{(x_1 - \xi_1)^3 - (x_1 - \xi_1)\xi_2^2}{r^4} \right] - 2 \cos 2\delta \left[\frac{(x_1 - \xi_1)^2 \xi_2}{r^4} \right] \mathrm{d}\Sigma, \\ u_2 &= \frac{s}{\pi} \int \sin 2\delta \left[\frac{\xi_2^3 - (x_1 - \xi_1)^2 \xi_2}{r^4} \right] + 2 \cos 2\delta \left[\frac{(x_1 - \xi_1)\xi_2^2}{r^4} \right] \mathrm{d}\Sigma, \end{aligned} \tag{3.57}$$

where

$$r^2 = (x_1 - \xi_1)^2 + \xi_2^2. \tag{3.58}$$

To perform the integration along the fault surface, we introduce a new coordinate η that runs along the fault surface. The coordinates of points on the fault are specified by

$$\begin{aligned} \xi_1 &= \eta \cos \delta, \\ \xi_2 &= -d - \eta \sin \delta, \end{aligned} \tag{3.59}$$

where d is the depth to the top of the fault. In this coordinate system, the distance from the fault to the observation point is

$$r^2 = (x_1 - \eta \cos \delta)^2 + (d + \eta \sin \delta)^2. \tag{3.60}$$

The fact that all of the terms in equation (3.57) have r^4 in the denominator makes integration difficult. The problem can be simplified greatly by adopting a coordinate system that is parallel and perpendicular to the fault, following Sato and Matsu'ura (1974). Define q as the coordinate perpendicular to the fault and p as the coordinate parallel to the fault (figure 3.9).

With reference to this figure, $\sin \delta$ is $q/(x + d \cot \delta)$, so that $q = x \sin \delta + d \cos \delta$, where for notational simplicity, we take $x \equiv x_1$. From figure 3.9, $r^2 = x^2 + d^2 = p^2 + q^2$. The fault parallel coordinate p is found by

$$\begin{aligned} p^2 = r^2 - q^2 &= r^2 - (x \sin \delta + d \cos \delta)^2, \\ &= x^2 \cos^2 \delta + d^2 \sin^2 \delta - 2xd \sin \delta \cos \delta, \\ &= (x \cos \delta - d \sin \delta)^2. \end{aligned} \tag{3.61}$$

In summary,

$$\begin{aligned} q &= x \sin \delta + d \cos \delta, \\ p &= x \cos \delta - d \sin \delta, \end{aligned} \tag{3.62}$$

and the inverse

$$x = p\cos\delta + q\sin\delta,$$
$$d = -p\sin\delta + q\cos\delta. \tag{3.63}$$

Introducing a new coordinate $\eta' = p - \eta$, the distance from a point on the fault to an observation point, from equation (3.60), is

$$\begin{aligned} r^2 &= [x - (p-\eta')\cos\delta]^2 + [d + (p-\eta')\sin\delta]^2, \\ &= x^2 + d^2 + (p-\eta')^2 - 2p(p-\eta'), \\ &= p^2 + q^2 + (p-\eta')^2 - 2p(p-\eta'), \\ &= q^2 + \eta'^2, \end{aligned} \tag{3.64}$$

which greatly simplifies the integration. If W is the downdip extent of slip, the limits of integration change from $\int_0^W d\eta$ to $\int_p^{p-W} d\eta'$. Expressing the integrals (3.57) in terms of η', we have

$$u_1 = -\frac{2s}{\pi}\int_p^{p-W} \frac{q\eta'(\eta'\cos\delta + q\sin\delta)}{(q^2+\eta'^2)^2} d\eta',$$
$$u_2 = -\frac{2s}{\pi}\int_p^{p-W} \frac{q\eta'(q\cos\delta - \eta'\sin\delta)}{(q^2+\eta'^2)^2} d\eta'. \tag{3.65}$$

These integrals are of the same form as those in equations (3.51) and (3.52), so equations (3.65) integrate to

$$u_1 = -\frac{s}{\pi}\left[\cos\delta\tan^{-1}\left(\frac{\eta'}{q}\right) - \frac{q\eta'\cos\delta + q^2\sin\delta}{q^2+\eta'^2}\right]_p^{p-W},$$
$$u_2 = \frac{s}{\pi}\left[\sin\delta\tan^{-1}\left(\frac{\eta'}{q}\right) + \frac{q^2\cos\delta - q\eta'\sin\delta}{q^2+\eta'^2}\right]_p^{p-W}. \tag{3.66}$$

For a single dislocation, let $W \to \infty$. Noting that $pq\cos\delta + q^2\sin\delta = x(d\cos\delta + x\sin\delta)$ and $q^2\cos\delta - qp\sin\delta = d(d\cos\delta + x\sin\delta)$, equation (3.66) becomes

$$u_1 = -\frac{s}{\pi}\left\{\cos\delta\left[-\frac{\pi}{2} - \tan^{-1}\left(\frac{p}{q}\right)\right] + \frac{x(d\cos\delta + x\sin\delta)}{x^2+d^2}\right\},$$
$$u_2 = \frac{s}{\pi}\left\{\sin\delta\left[-\frac{\pi}{2} - \tan^{-1}\left(\frac{p}{q}\right)\right] - \frac{d(d\cos\delta + x\sin\delta)}{x^2+d^2}\right\}. \tag{3.67}$$

Note from figure 3.9 that the following angles sum to π:

$$[\pi/2 - \tan^{-1}(p/q)] + \tan^{-1}(x/d) + (\pi/2 - \delta) = \pi, \tag{3.68}$$

where the three terms identify the three angles indicated in figure 3.9. Thus,

$$u_1 = \frac{s}{\pi}\left\{\cos\delta[\tan^{-1}(x/d) - \delta + \pi/2] - \frac{x(d\cos\delta + x\sin\delta)}{x^2+d^2}\right\},$$
$$u_2 = -\frac{s}{\pi}\left\{\sin\delta[\tan^{-1}(x/d) - \delta + \pi/2] + \frac{d(d\cos\delta + x\sin\delta)}{x^2+d^2}\right\}. \quad (3.69)$$

Once again, we can remove rigid body terms. In this case, subtract $(s/\pi)[(\pi/2 - \delta)\cos\delta - \sin\delta]$ from the horizontal displacement and $(s/\pi)(\delta - \pi/2)\sin\delta$ from the vertical. This yields

$$\boxed{\begin{aligned} u_1(x_1, x_2 = 0) &= \frac{s}{\pi}\left[\cos\delta\tan^{-1}(\zeta) + \frac{\sin\delta - \zeta\cos\delta}{1+\zeta^2}\right], \\ u_2(x_1, x_2 = 0) &= -\frac{s}{\pi}\left[\sin\delta\tan^{-1}(\zeta) + \frac{\cos\delta + \zeta\sin\delta}{1+\zeta^2}\right], \end{aligned}} \quad (3.70)$$

where the parameter ζ is the distance from the dislocation scaled by the depth,

$$\zeta \equiv \frac{x_1 - \xi_1}{d}. \quad (3.71)$$

Note that as written here, $s > 0$ corresponds to normal faulting for $0 \le \delta \le \pi/2$ and reverse faulting for $\pi/2 \le \delta \le \pi$, while the opposite sense follows for $s < 0$.

Last, the surface parallel normal strain is

$$\epsilon_{11}(x_1, x_2 = 0) = \frac{\partial}{\partial x_1}u_1(x_1, x_2 = 0) = \frac{2s}{\pi d}\left[\frac{\zeta^2\cos\delta - \zeta\sin\delta}{(1+\zeta^2)^2}\right]. \quad (3.72)$$

Equations (3.70) apply to the edge dislocation geometry shown in figure 3.8. In order to model uniform slip over a confined interval, we superimpose two dislocations with opposite sign at either end of the fault surface. For a dislocation that breaks the surface, take a positive dislocation at $\xi_1 = 0$, $d = 0$, a negative dislocation at $\xi_1 = x_d \equiv d/\tan\delta = L\cos\delta$, and depth d, where L is the downdip length of the fault. Taking the limit of equations (3.70) as $d \to 0$, the only nonzero terms are the arctangents, which go to $\pi/2\ \mathrm{sgn}(\zeta)$ in the limit. Here sgn(z) gives the sign of z. Thus, the displacements for a surface breaking dislocation are, taking $\xi_1 = x_d$ so that $\zeta = (x_1 - x_d)/d$,

$$\boxed{\begin{aligned} u_1(x_1, x_2 = 0) &= -\frac{s}{\pi}\left\{\cos\delta\left[\tan^{-1}(\zeta) - (\pi/2)\,\mathrm{sgn}(x)\right] + \frac{\sin\delta - \zeta\cos\delta}{1+\zeta^2}\right\}, \\ u_2(x_1, x_2 = 0) &= \frac{s}{\pi}\left\{\sin\delta\left[\tan^{-1}(\zeta) - (\pi/2)\,\mathrm{sgn}(x)\right] + \frac{\cos\delta + \zeta\sin\delta}{1+\zeta^2}\right\}. \end{aligned}} \quad (3.73)$$

3.4 Coseismic Deformation Associated with Dipping Faults

The displacements and horizontal strain due to a 20-degree dipping thrust fault are shown in figure 3.10. The geometry is characteristic of large subduction zone earthquakes. Note that

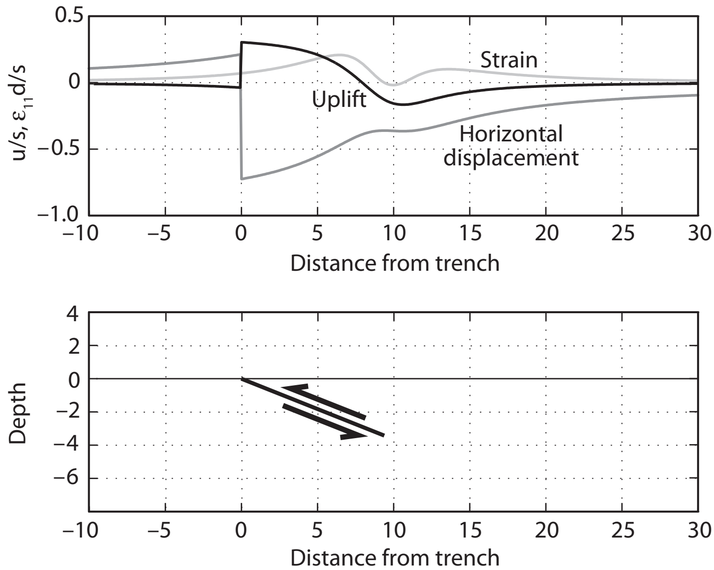

Figure 3.10. Coseismic deformation for a thrust fault. The top panel shows the horizontal and vertical displacements and the horizontal strain. The bottom panel shows the fault geometry.

the horizontal displacement is negative, meaning directed toward the fault, on the hanging-wall side of the fault and positive on the foot-wall side. There is uplift at the fault on the hanging wall, but subsidence above the downdip end of the fault. Generally, we anticipate tilting of the land away from the trench, except landward of the downdip projection of the fault, which tilts toward the trench. The horizontal strain is extensional, due to elastic rebound of stored compression, except for a small region above the downdip end of the fault. For most subduction zone earthquakes, much of the displacement field is underwater and therefore difficult to measure. There are many excellent comparisons between observations and model predictions for stations on the hanging wall of subduction earthquakes.

Data exist on both sides of the fault for continental thrust events. For example, the 20 September 1999 Chi-Chi, Taiwan, earthquake ($M_W = 7.6$) generated very large displacements that were measured with high accuracy using GPS. The earthquake occurred along the north–south trending Chelungpu fault (Kao and Chen 2000) and resulted in 2,440 fatalities, over 11,000 injuries, and the collapse of at least 50,000 structures. Coseismic displacements were determined by Yu et al. (2001) at 128 stations of the Taiwan GPS Network. The horizontal coseismic displacements increase from 1 m at the southern end of the fault to 9 m at the northern end (figure 3.11).

The vertical offsets (not shown) were largest near the fault trace, where the hanging wall was uplifted as much as 4.4 meters at the northern end of the rupture (plate 1), and decrease rapidly toward the east. The stations on the foot-wall side show smaller amounts of subsidence ranging from 0.02 to 0.32 meter. Net displacements at the ground surface range up to nearly 12 meters, at the northwest corner of the rupture. Along the north–south trending fault trace, the ground is warped into a monoclinal flexure indicative of shallow thrusting. Aftershocks illuminate a fault that dips 20 to 30 degrees to the east (Kao and Chen 2000).

Because the strike of the main rupture was nearly north–south, we compare the east and vertical components of the displacement field to predictions of a plane strain model (figure 3.12). In actuality, the Chi-Chi earthquake involved a significant amount of oblique